Identification of common genes of rhinovirus single/double-stranded RNA-induced asthma deterioration by bioinformatics analysis

QIAN AN[1], YI CAO[2], WEI GUO[2], ZIYUN JIANG[2], HUI LUO[2], HUI LIU[2] and XIAODONG ZHAN[2]

[1]Department of Respiratory and Critical Care Medicine, Wuhu Hospital of Traditional Chinese Medicine, Wuhu, Anhui 241000; [2]Department of Medical Parasitology, School of Basic Medicine, Wannan Medical College, Wuhu, Anhui 241002, P.R. China

Received August 28, 2023; Accepted January 29, 2024

DOI: 10.3892/etm.2024.12498

Abstract. Rhinovirus (RV) is the most common respiratory virus affecting humans. The majority of asthma deteriorations are triggered by RV infections. However, whether the effects of RV single- and double-stranded RNA on asthma deterioration have common target genes needs to be further studied. In the present study, two datasets (GSE51392 and GSE30326) were used to screen for common differentially expressed genes (cDEGs). The molecular function, signaling pathways, interaction networks, hub genes, key modules and regulatory molecules of cDEGs were systematically analyzed using online tools such as Gene Ontology, Kyoto Encyclopedia of Genes and Genomes, STRING and NetworkAnalyst. Finally, the hub genes STAT1 and IFIH1 were verified in clinical samples using reverse transcription-quantitative PCR (RT-qPCR). A total of 85 cDEGs were identified. Function analysis revealed that cDEGs served an important role in the innate immune response to viruses and its regulation. Signal transducer and activator of transcription 1 (STAT1), interferon induced with helicase C domain 1 (IFIH1), interferon regulatory factor 7 (IRF7), DExD/H box helicase 58 (DDX58) and interferon-stimulating gene 15 (ISG15) were detected to be hub genes based on the protein-protein interactions and six topological algorithms. A key module involved in influenza A, the Toll-like receptor signaling pathway, was identified using Cytoscape software. The hub genes were regulated by GATA-binding factor 2 and microRNA-146a-5p. In addition, RT-qPCR indicated that the expression levels of the hub genes STAT1 and IFIH1 were low during asthma deterioration compared with post-treatment recovery samples. The present study enhanced the understanding of the mechanism of RV-induced asthma deterioration.

Introduction

Allergic asthma is a common respiratory disease in clinical practice. Its main pathogenesis involves the production of specific IgE antibodies, chronic airway inflammation, airway remodeling and airway hyperresponsiveness during the response of the immune system to environmental allergens (1,2). The most important link in the pathogenesis of asthma is allergic sensitization through the activation of respiratory epithelial cells (3). In recent years, the incidence and prevalence of allergic asthma have rapidly increased, particularly in low and middle income countries (4,5). Respiratory viral infections are the most common cause of allergic asthma deteriorations (6).

Rhinovirus (RV) is a single-stranded RNA (ssRNA) virus of the picornavirus family, the most common human respiratory virus and is considered to be the main pathogen causing asthma deterioration (7,8). In children, 80% of asthma deteriorations are caused by RV infections (9). It has been demonstrated that cadherin-related family member 3 (CDHR3), a specific cell marker of ciliated cells, is a risk gene for asthma deterioration induced by RV in children (10). Additionally, repeated RV infection can promote airway remodeling by upregulating TNF superfamily member 14, IL-1β and TGF-β, even in the absence of allergens (11). Notably, double-stranded RNA (dsRNA) generated by RV in the process of replication can also cause a strong immune response of the host (12). Airway epithelial cells are the primary target for RV and the first line of defense in the immune response (13). A study has shown that ssRNA infection in epithelial cells mainly activates the interferon-induced antiviral signaling pathway with interferon regulatory factor (IRF) 7 (14). The mechanism through which dsRNA infects and induces antiviral immune responses in

Correspondence to: Professor Xiaodong Zhan, Department of Medical Parasitology, School of Basic Medicine, Wannan Medical College, 22 Wenchang West Road, Wuhu, Anhui 241002, P.R. China
E-mail: xdzhan@126.com

Abbreviations: RV, rhinovirus; ssRNA, single-stranded RNA; dsRNA, double-stranded RNA; cDEG, common differentially expressed gene; GO, Gene Ontology; KEGG, Kyoto Encyclopedia of Genes and Genomes; PPI, protein-protein interaction; TF, transcription factor

Key words: RV, asthma deteriorations, hub genes, bioinformatics

upper and lower respiratory tract epithelial cells is similar; however, the induction of interferon-related genes (such as IRF3, interferon-α/β receptor 1 and interferon β1) is impaired in patients with asthma (15). RV-induced asthma deterioration is a complex pathological process involving a large number of gene expression changes and signaling pathways (7,12,14,15). However, it is so far unknown, whether there is a common target and regulatory network of rhinovirus single and double stranded RNA inducing asthma deterioration.

Bioinformatics analysis is a powerful tool used to explore the key genes and molecular regulatory networks in pathogenesis (16). In the present study, common differentially expressed genes (cDEGs) of asthma deterioration induced by RV dsRNA and ssRNA were screened using bioinformatics analysis. The functions of the proteins encoded by the cDEGs and their interaction networks were analyzed using Gene Ontology (GO) and Kyoto Encyclopedia of Genes and Genomes (KEGG), and protein-protein interaction (PPI) analyses, respectively. Hub genes were identified and validated. The hub genes and regulatory networks identified in the present study may not only help comprehend the molecular mechanism of RV-induced asthma deterioration, but also serve as potential targets to improve treatment.

Materials and methods

Clinical samples and ethics. A total of eight clinical samples (paired sample, the comparison of the deterioration and recovery periods) were collected from pediatric patients with RV-induced asthma deterioration between May 2022 and August 2022. The patients included five boys and three girls (mean age, 13 years). Sterile cytology brushes were used to collect airway epithelium and secretions from the posterior surface of the inferior turbinate from patients at Wuhu Hospital of Traditional Chinese Medicine (Wuhu, China). Collected brushes were immediately submerged in RLT Plus lysis buffer (cat. no. 1053393; Qiagen GmbH) with β-mercaptoethanol (cat. no. 444203; MilliporeSigma) and frozen at -80˚C for subsequent experiments. The inclusion criteria for the samples used in the present study were established by referring to relevant literature (17): RV nucleic acid test (+) using the human Rhv ELISA kit (cat. no. YJ711802; Shanghai Enzyme-linked Biotechnology Co., Ltd.), proportion of eosinophils >5% using blood cell analyzer (XS-1800; Sysmex America, Inc.), bronchial dilation test (forced expiratory volume of first second) >12% (MasterScreen IOS; Erich Jaeger GmbH), chest tightness, cough and diffuse wheezes in both lungs, and all other respiratory diseases ruled out. Samples were collected from each of the 8 patients at both timepoints during the asthma attacks and 14 days after the symptoms had disappeared with treatment. The present study was approved by the Ethics Committee of Wuhu Hospital of Traditional Chinese Medicine (approval no. 20220430; Wuhu, China).

Retrieval of datasets. In the present study, two datasets (GSE30326 and GSE51392) were downloaded from the Gene Expression Omnibus (GEO) database (https://www.ncbi.nlm.nih.gov/geo/) (14,15). The characteristics of the patients in these two datasets are presented in Table I. GSE30326 analyzed gene expression profiles in nasal lavage samples of 16 asthmatic children during acute RV ssRNA-induced deterioration and after 7-14 days. The cellular composition of the acute samples was macrophages (83.9±2.7%), neutrophils (12.3±2.5%), epithelial cells (2.2±1.0%) and eosinophils (1.6±0.5%). The recovery period samples contained macrophages (72.1±4.8%), epithelial cells (16.6±4.7%), neutrophils (9.1±1.2%) and eosinophils (1.7±0.8%). In GSE30326, a network of susceptible genes was constructed using the weighted gene co-expression network analysis algorithm (14). The GSE51392 dataset was used to identify microarray gene expression profiles of RV dsRNA-treated nasal and bronchial epithelial cells from the same individual. A total of 6 patients with asthma induced by RV dsRNA and 6 healthy controls from the GSE51392 dataset (5 samples were involved in allergic rhinitis and were excluded due to weak correlation with this study) were selected as the study sample (15). The susceptibility genes in the aforementioned two datasets were identified by moderated t statistics, and genes that were significantly modulated at a false discovery rate adjusted $P<0.05$ were used for further experiments.

Screening and functional annotation of cDEGs. The flowchart of the present study is shown in Fig. 1. First, cDEGs from the GSE30326 and GSE51392 datasets were analyzed using GEO2Rweb (https://www.ncbi.nlm.nih.gov/geo/geo2r). The cut-off criteria were: Adjusted $P<0.05$ and $\log_2$-fold change >1.5 or <-1.5. Second, the cDEGs were visualized using ggplot2 (version 3.3.3; https://cran.r-project.org/mirrors.html), and functional annotation was performed using GO and KEGG pathway analysis [clusterProfiler (version 4.4.4) R package (version 4.2.1); http://bioconductor.org/packages/release/bioc/html/clusterProfiler.html].

Screening hub genes and key module. The PPI network of DEGs was constructed using the STRING database (https://cn.string-db.org/). PPIs were analyzed using Cytoscape software (https://cytoscape.org/; version 3.8.2), and the hub genes were evaluated based on the score of topological algorithms in Cytoscape, including the BottleNeck, closeness, degree, density of maximum neighborhood component, EcCentricity and maximal clique centrality algorithms. In addition, the key modules from the PPI network were analyzed using the Molecular Complex Detection plugin in Cytoscape. The functional annotation of key module were performed using GO-KEGG database.

Identification of candidate regulators of hub genes. The regulators of hub genes [including transcription factors (TFs), microRNAs (miRNAs/miRs) and drugs] were screened through online resources, such as NetworkAnalyst (version 3.0; https://www.networkanalyst.ca/) and DSigDB (https://amp.pharm.mssm.edu/Enrichr/).

Reverse transcription-quantitative PCR (RT-qPCR). Total RNA was extracted from each sample using TRNzol Universal Reagent (cat. no. DP424; Tiangen Biotech Co., Ltd.) according to the manufacturer's instructions. Chloroform was added to separate the organic and inorganic phases, RNA was precipitated with isopropanol and washed with 75% ethanol. The RNA concentration (A260/280) was measured using a spectrophotometer (Nanodrop; Thermo Fisher Scientific,

Table I. Patient characteristics for the two datasets (GSE30326 and GSE51392).

GEO Accession	GSE30326	GSE51392
Subjects	16 children	17 adults
Mode of pairing	Acute phase vs. remission phase	Allergic asthma vs. healthy controls
RNA type	Single-stranded RNA	Double-stranded RNA
RNA identification method	Reverse transcription-quantitative PCR	Poly(I:C), a synthetic double-stranded RNA
Experimental design	Differentially expressed genes in respiratory epithelial cells between acute exacerbation and remission were analyzed using a gene chip	Microarray identification of double-stranded RNA-induced gene expression profiles in respiratory epithelial cells
Sample source	Nasal cavity	Nasal cavity and bronchi, paired samples
Predicted FEV1 at remission, %	103.4±10.9	109±11.0
Allergen skin test positive, %	68.7	100

FEV1, forced expiratory volume of first second.

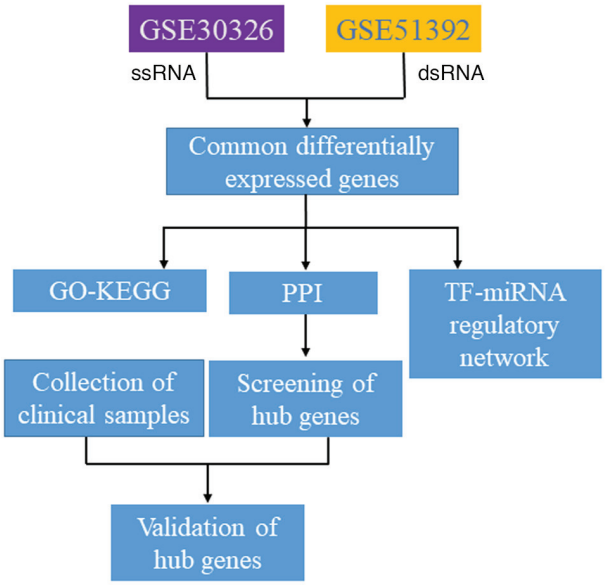

Figure 1. Flowchart of the present study. ssRNA, single-stranded RNA; dsRNA, double-stranded RNA; GO, Gene Ontology; KEGG, Kyoto Encyclopedia of Genes and Genomes; PPI, protein-protein interaction; TF, transcription factor; miRNA, microRNA.

Inc.). Next, 1 μg RNA was reverse transcribed using HiScript II Q RT SuperMix (cat. no. R222-01; Vazyme Biotech Co., Ltd.). Temperature protocol of reverse transcription: 50˚C for 15 min; 85˚C for 5 sec. Quantification of signal transducer and activator of transcription 1 (STAT1) and interferon induced with helicase C domain 1 (IFIH1) expression was performed using a Real-Time PCR Detection System (LightCycler 96; Roche Diagnostics). Reactions were performed in three replicates with 2 μl cDNA per reaction using the 2XSG Fast qPCR Master Mix (cat. no. B639273; Sangon Biotech Co., Ltd.). Thermocycling conditions were as follows: 3 min at 95˚C and 30 sec at 60˚C, for 40 cycles. The primers were: STAT1 forward, 5'-GCTTGACAATAAGAGAAAGG-3' and reverse, 5'-CGCTCTGCTGTCTCCGCTTCCACTCC-3'; IFIH1 forward, 5'-GTTGAAAAGGCTGGCTGAAAAC-3' and reverse, 5'-TCGATAACTCCTGAACCACTG-3'; and GAPDH forward, 5'-GAAGGTGAAGGTCGGAGTC-3' and reverse, 5'-GAAGATGGTGATGGGATTTCC-3'. All primers were synthesized by TsingKe Biological Technology. Relative gene expression was calculated using the $2^{-\Delta\Delta Cq}$ method (18). GAPDH was used as the internal reference.

Statistical analysis. SPSS (version 20; IBM Corp.) was utilized for statistical analysis of three technical replicates per sample. The paired t-test was used to compare differences in mRNA expression levels. Data are shown as mean ± standard deviation. $P<0.05$ was considered to indicate a statistically significant difference.

Results

Identification of cDEGs between GSE51392 and GSE30326. In the GSE51392 dataset, 1,075 DEGs were identified. Among them, 337 genes were upregulated and 738 downregulated. In the GSE30326 dataset, a total of 198 DEGs were identified and all of them were downregulated. Of note, a total of 85 cDEGs were identified in the aforementioned two datasets (Fig. 2).

Functional enrichment analysis of cDEGs. To understand the functions of the cDEGs, GO and KEGG pathway analysis was carried out using the Enrichr web server and KEGG Mapper, respectively. GO analysis revealed enrichment for 'response to virus', 'double-stranded RNA binding' and 'single-stranded RNA binding'. In addition, KEGG pathway analysis revealed enrichment of cDEGs associated with 'influenza A', 'hepatitis C' and 'NOD-like receptor signaling pathway'. More detailed functional enrichment information of DEGs is presented in Table II.

PPI network analysis. The 85 cDEGs were analyzed using the STRING online tool and the result is shown in Fig. 3. The analyzed network had 85 nodes and 996 edges. The average node degree was 23.4, and the average local clustering coefficient was 0.648.

Table II. GO-KEGG enrichment analysis for common differentially expressed genes.

Terms	ID	Description	GeneRatio	Adjusted P-value
GO				
BP	GO:0009615	Response to virus	39/79	$1.59x10^{-41}$
BP	GO:0051607	Defense response to virus	35/79	$4.89x10^{-40}$
BP	GO:0140546	Defense response to symbiont	35/79	$4.89x10^{-40}$
BP	GO:0002831	Regulation of response to biotic stimulus	25/79	$9.69x10^{-22}$
BP	GO:1903900	Regulation of viral life cycle	17/79	$3.54x10^{-18}$
MF	GO:0003725	Double-stranded RNA binding	10/80	$1.8x10^{-10}$
MF	GO:0003727	Single-stranded RNA binding	7/80	$1x10^{-5}$
MF	GO:0004842	Ubiquitin-protein transferase activity	12/80	$2.36x10^{-5}$
MF	GO:0019787	Ubiquitin-like protein transferase activity	12/80	$3.22x10^{-5}$
MF	GO:0003724	RNA helicase activity	6/80	$3.49x10^{-5}$
KEGG	hsa05164	Influenza A	13/49	$9.93x10^{-10}$
KEGG	hsa05160	Hepatitis C	10/49	$8.63x10^{-7}$
KEGG	hsa04621	NOD-like receptor signaling pathway	9/49	$2.78x10^{-5}$
KEGG	hsa05162	Measles	8/49	$2.78x10^{-5}$
KEGG	hsa04622	RIG-I-like receptor signaling pathway	6/49	$5.15x10^{-5}$

GO, Gene Ontology; KEGG, Kyoto Encyclopedia of Genes and Genomes; BP, biological process; MF, molecular function; NOD, nucleotide oligomerization domain; RIG-I, retinoic acid-inducible gene I.

Figure 2. Venn diagram of common differentially expressed genes from the two datasets.

Detection of hub genes and module analysis. According to topology analysis, five cDEGs [STAT1, IFIH1, IRF7, DExD/H box helicase 58 (DDX58) and interferon-stimulating gene 15 (ISG15)] were considered to be hub genes (Table III). The proteins encoded by the hub genes have rich interactions with other proteins, including 118 nodes and 1,531 edges (Fig. 4). Module analysis demonstrated that immune-responsive gene 1 (IRG1), basic leucine zipper transcription factor 2 (BATF2) and epithelial stromal interaction 1 were high density modules and had significant interactions with hub genes (Fig. 5). The genes in the module were mainly enriched in 'influenza A', 'Toll-like receptor signaling pathway', 'coronavirus disease-COVID-19', 'hepatitis B' and 'herpes simplex virus 1 infection' signaling pathways (Table IV).

TF regulatory network analysis of hub genes. A total of 18 TFs critical for regulating the expression of hub genes were identified using NetworkAnalyst. Among them, GATA-binding factor 2 (GATA2) was found to regulate the STAT1, DDX58 and ISG15 hub genes, and CAMP responsive element binding protein 1 (CREB1) was found to regulate STAT1, IFIH1 and ISG15 (Fig. 6A). In addition, 25 miRNAs critical for regulating the expression of hub genes were identified. In the regulatory network, miR-146a-5p regulated the STAT1, IRF7 and ISG15 hub genes. IFIH1 was mainly regulated by miR-424-5p (Fig. 6B).

Screening of potential therapeutic drugs. Enrichr Platform analysis revealed that suloctidil, 3'-Azido-3'-deoxythymidine, estradiol and acetaminophen were potential therapeutic targets for cDEGs and hub genes (Table V).

Validation of key hub genes. RT-qPCR was used to validate the mRNA expression of the hub genes STAT1 and IFIH1, and it was revealed that the mRNA expression levels of STAT1 were downregulated in asthma deterioration samples compared with post-treatment recovery samples, and the mRNA expression levels of IFIH1 exhibited the same trend (Fig. 7; $P<0.01$).

Discussion

The two datasets involved in the present study revealed that both STAT1 and IFIH1 were significantly downregulated in respiratory epithelial cells infected with RV ssRNA or dsRNA. Network analysis demonstrated that STAT1 and IFIH1 served important roles in key modules as hub genes. Finally, it was found that the expression levels of these two genes were significantly higher in the recovery phase than in the deterioration

Table III. Ranking of the top 5 genes based on 6 algorithms.

Degree	MCC	DMNC	EcCentricity	Closeness	BottleNeck
STAT1	IFIH1	HERC6	STAT1	STAT1	STAT1
IFIH1	RSAD2	IFI6	IFIH1	IFIH1	HELZ
IRF7	IFIT3	HERC5	RSAD2	IRF7	PRKCA
DDX58	STAT1	EPSTI1	IFI35	ISG15	XIAP
ISG15	MX1	SAMD9	USP18	DDX58	MX1

MCC, maximal clique centrality; DMNC, density of maximum neighborhood component.

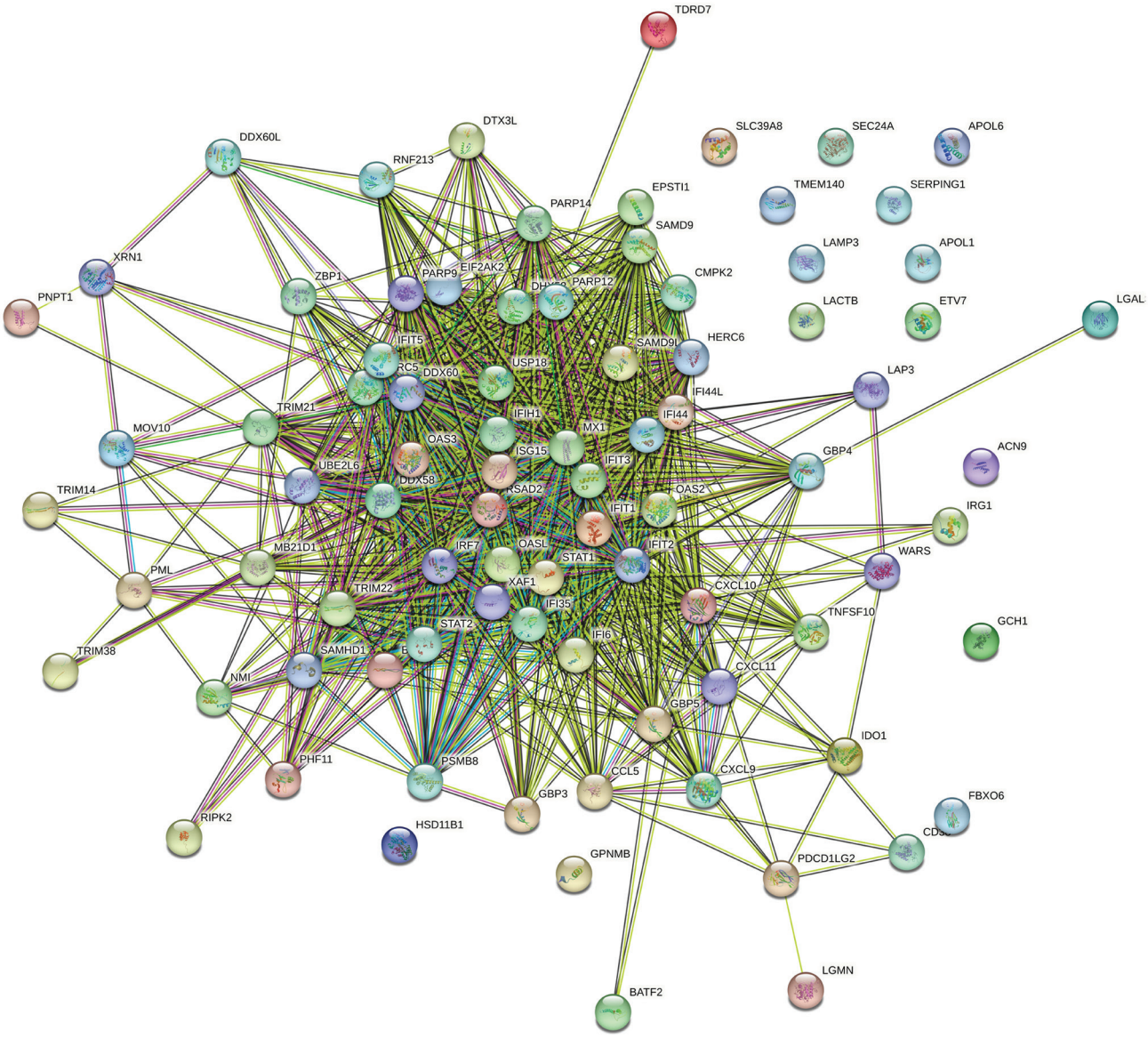

Figure 3. PPI network for identified cDEGs. Nodes indicate cDEGs and edges represent protein-protein associations. PPI enrichment P<1.0x10^{-16}. cDEGs, common differentially expressed genes; PPI, protein-protein interaction.

phase in clinical samples, suggesting that they can be used as potential therapeutic targets to improve asthma deteriorations caused by RV ssRNA or dsRNA. Studies have shown that STAT1 is an important TF that maintains T helper 1 (Th1) cell development and serves an important role in regulating asthma deterioration; low levels of STAT1 increase the risk of asthma attacks and virus susceptibility (19,20). STAT1 is necessary to control the replication of influenza A *in vivo* and serves a crucial role in the Toll-like receptor (TLR) signaling pathway-mediated inflammatory response (21,22). In the

Table IV. Analysis of the signaling pathways associated with the genes within the key module.

ID	Description	Adjusted P-value	Gene ID
hsa05164	Influenza A	$6.8x10^{-6}$	OAS2/RSAD2/STAT1/IRF7/IFIH1
hsa04620	Toll-like receptor signaling pathway	$7.2x10^{-5}$	CXCL11/CXCL9/STAT1/IRF7
hsa05171	Coronavirus disease-COVID-19	$0.1x10^{-3}$	OAS2/ISG15/STAT1/IFIH1
hsa05161	Hepatitis B	0.004	STAT1/IRF7/IFIH1
hsa05168	Herpes simplex virus 1 infection	0.034	OAS2/STAT1/IRF7/IFIH1

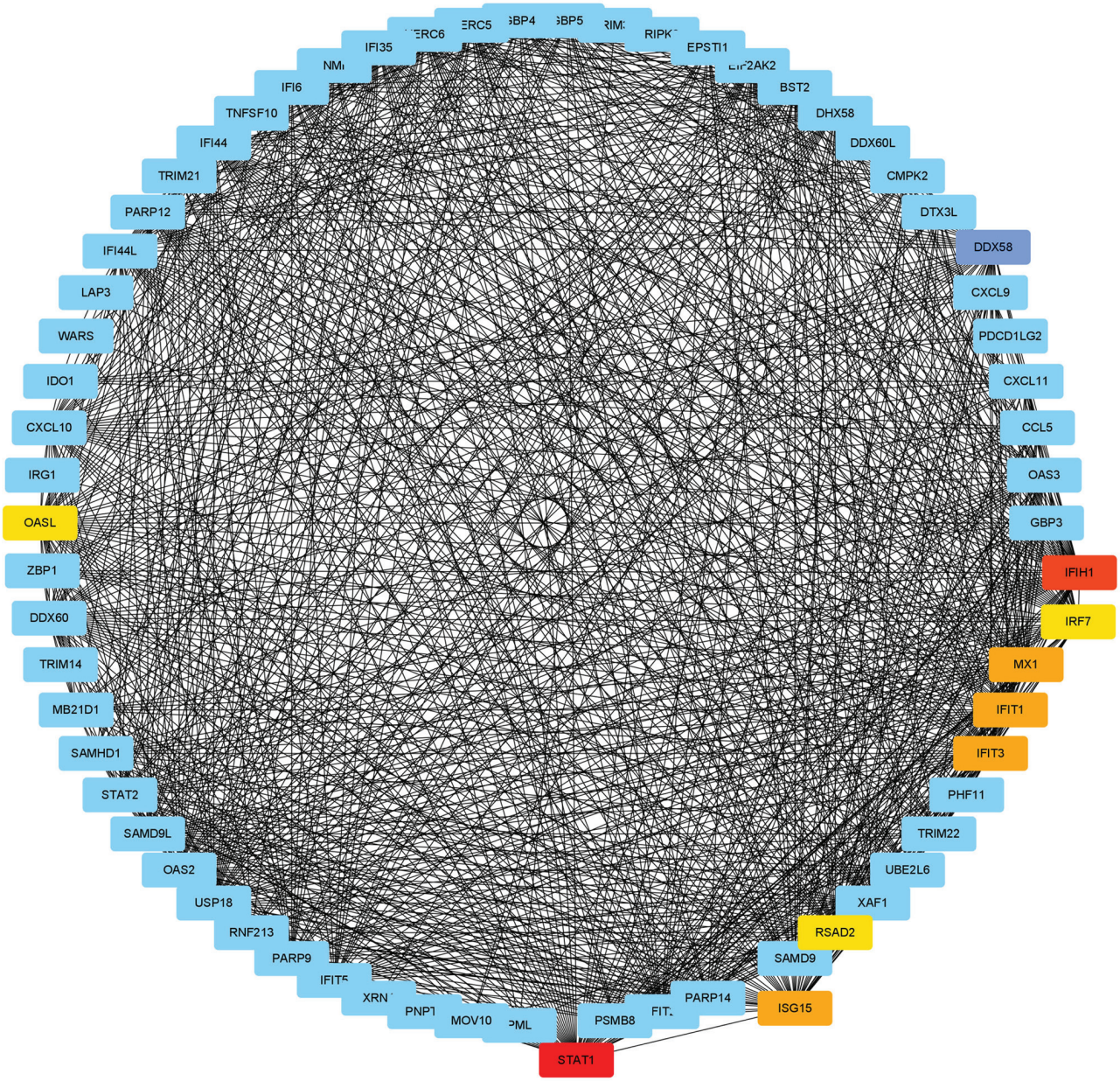

Figure 4. Detection of hub genes from the protein-protein interaction network of common differentially expressed genes. Red indicates that the gene has the highest degree value, orange indicates that the gene has a lower degree value than red and blue indicates that the gene has a lower degree value than orange.

course of COVID-19, STAT1 is dysfunctional and enhancing the activity of STAT1 has a therapeutic effect (23). A study has shown that eosinophils in the airway of allergic asthma enhanced the antiviral immune response to influenza A by upregulating IFIH1 transcription (24). IFIH1 can recognize and bind to dsRNA produced in the process of viral replication (25). TLR can recognize ssRNA in the nucleus and bind with dsRNA and synergistically mediate congenital antiviral

Table V. Potential drug components for treatment of rhinovirus-induced asthma exacerbation.

Component	Overlap	Adjusted P-value	Odds ratio	Combined score	Target genes
Suloctidil	38/141	$6.85x10^{-57}$	146.1635	19919.95	IFIT5, IFI6, IFIT1, IFI44L, IFIT3, IFIT2, OASL, IFIH1, IFI44, EIF2AK2, ISG15, CXCL10, CXCL11, AIM2, OAS2, OAS3, TFEC, IRF7, C19ORF66, CD69, XAF1, SP140L, IRF9
3'-Azido-3'-deoxythymidine	27/374	$2.15x10^{-23}$	24.95654	1436.213	SAMD9L, IFIT5, IFI6, DDX60L, IFIT1, IFI44L, IFIT2, IFIH1, CASP5, LAMP3, C3AR1, EPSTI1, TNFSF10, LGALS9, TRIM22, STAT1, MX1, ISG15
Estradiol	45/4336	$6.29x10^{-8}$	3.809732	78.47791	IFIT5, IFI6, UBE2L6, DDX60L, IFIT1, TARP, IFI44L, IFIT3, IFIT2, IFIH1, DDX58, STAT1, P2RY14, CYBB, IFI44, EIF2AK2, ISG15, NMI, PARP9, CXCL10, CXCL11, OAS2, OAS3, IRF7, CMPK2, XAF1, HAMP, IRF9
Acetaminophen	43/4135	$1.74x10^{-7}$	3.694254	71.97291	IFI6, TMEM51, UBE2L6, DDX60L, IFIT1, IFIT3, IFIT2, IFIH1, PSTPIP2, LAMP3, C3AR1, TNFSF10, NBN, TRIM21, TRIM22, GBP4, TNS1, GBP3, RSAD2, DYNLT1, DDX58, STAT1, SPHK1, PHF11, MX1, IFI44, EIF2AK2, NMI, RNASE2, PARP9, PATL1, IRF9

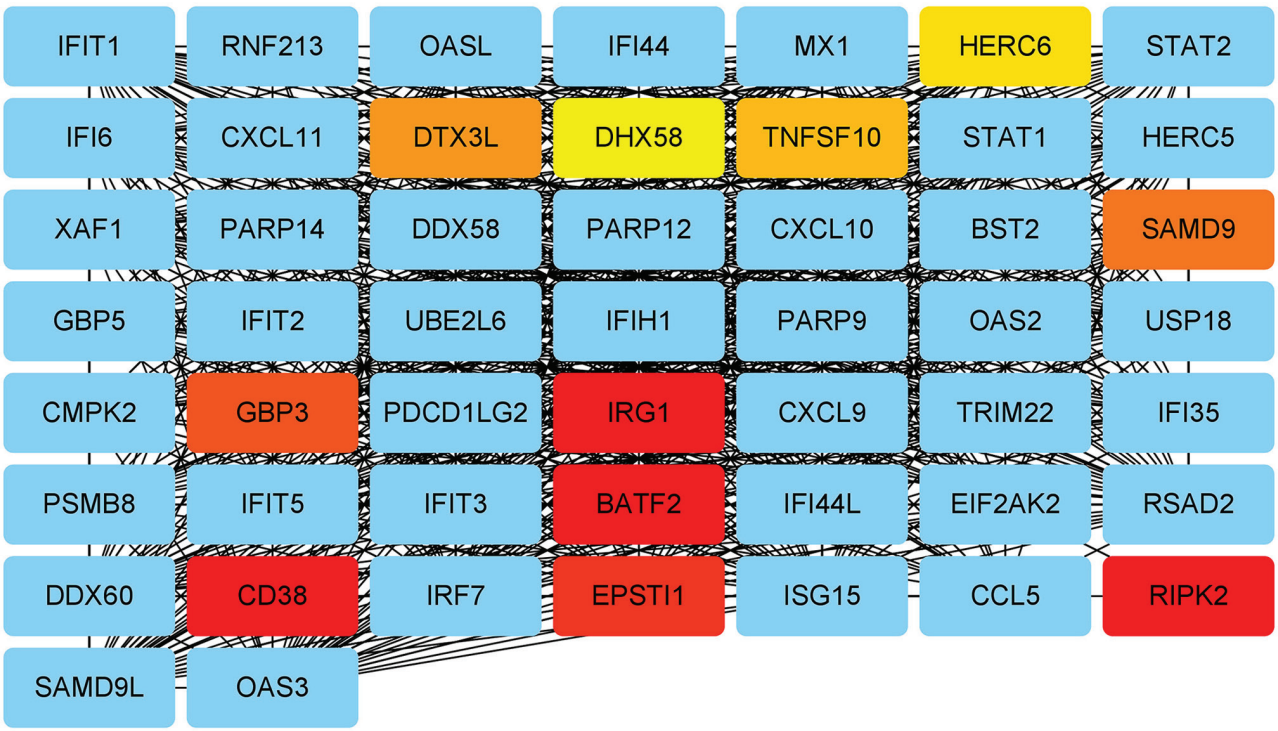

Figure 5. Module analysis network obtained from PPI network. The network represents highly interconnected regions of the PPI network. Red represents a high clustering coefficient across the PPI network. Different colors indicate different clustering coefficients. Brown, yellow, light yellow and blue represent the gradually decreasing clustering coefficients. PPI, protein-protein interaction.

immune response with IFIH1 (26). Studies have shown that there are two alleles of IFIH1 in the pathogenesis of COVID-19: The patients with rs1990760/IFIH1 exhibit an attenuated inflammatory response and improved outcomes, while patients with rs19907601/IFIH1 exhibit poor prognosis (27,28). In addition, IFIH1/DDX58 is the primary cytoplasmic sensor for the intracellular detection of viral pathogen-associated molecular patterns of viral RNA (29). It is an important component in the formation of cytoplasmic RNA-binding protein complement, which contributes to innate antiviral immunity (30). IFIH1/DDX58 expression in epithelia of the upper airway is higher in children than in adults, resulting in stronger

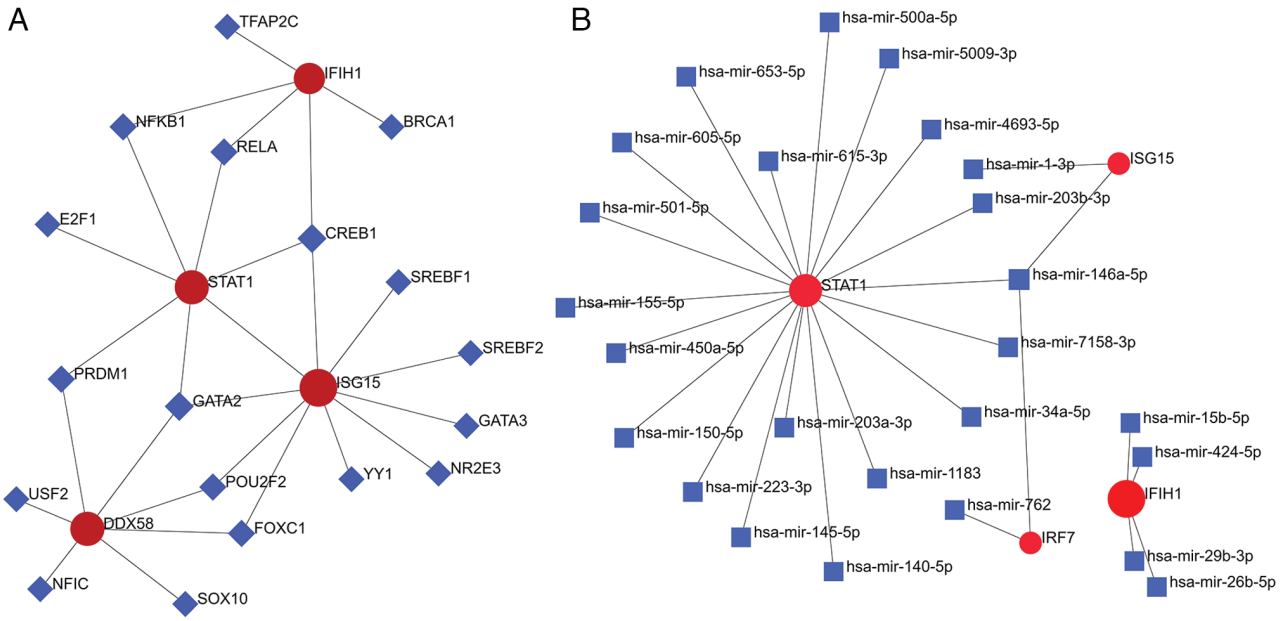

Figure 6. Regulatory network of TFs and miRNAs for hub genes. (A) Regulatory network of TFs for hub genes. The red color nodes represent the hub genes, and the blue color nodes represent TFs. (B) Regulatory network of miRNAs for hub genes. The red color nodes represent the hub genes and the blue color nodes represent miRNAs. TF, transcription factor; miRNA/mir, microRNA.

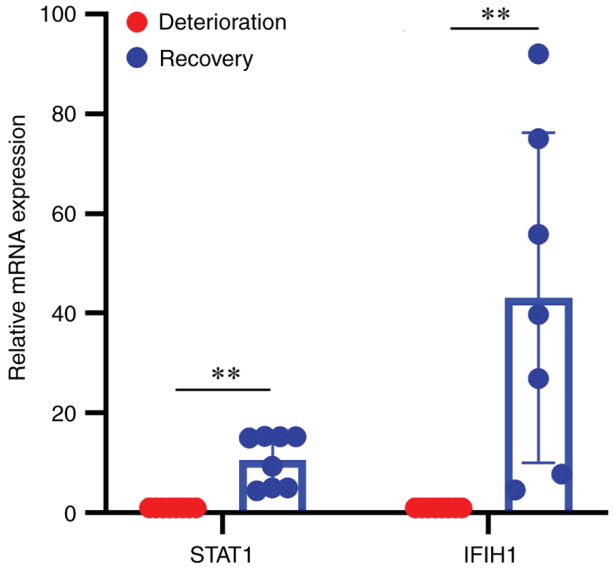

Figure 7. Reverse transcription-quantitative PCR results of STAT1 and IFIH1 mRNA expression. n=8. **P<0.01. IFIH1, interferon induced with helicase C domain 1; STAT1, signal transducer and activator of transcription 1.

early innate antiviral immunity to severe acute respiratory syndrome coronavirus 2 (SARS-CoV-2) infection in children (31). Low IFIH1/DDX58 expression in patients with viral infection predicts poor prognosis (32). These previous results were consistent with those of the present study (that STAT1 and IFIH1 were downregulated during asthma deterioration).

In the two datasets involved in the present study, IFIH1 is more downregulated than STAT1 during RV-induced asthma deteriorations (14,15). This may be due to two reasons. Firstly, asthma exhibits an imbalance of Th1/Th2 cells in cytology and Th2 cells increase during asthma attacks (33), which reduces the generation of Th1 cytokine interferon, causing a deficiency in antiviral response and increase in viral load in patients with asthma (34). Secondly, IgE antibodies eliminate the biological activity of interferon α and reduce its concentration and antiviral ability (35). GO-KEGG enrichment analysis showed that cDEGs were mainly involved in '(defense) response to virus', 'regulation of viral life cycle', 'double-stranded RNA binding and 'single-stranded RNA binding', as well as in 'influenza A' and 'NOD-like receptor signaling pathway'. A previous study has shown that the nucleotide oligomerization domain (NOD)-like receptor signaling pathway mediates airway epithelial inflammation and mucus production, which is an important mechanism of RV-induced airway remodeling (36). Dataset analysis showed that the genes with ds/ssRNA binding functions [such as DExD/H-box 60 like (DDX60L) and polyribonucleotide nucleotidyltransferase 1 (PNPT1)] were significantly reduced (14,15). DDX60L is an interferon-stimulated gene product, which can effectively inhibit viral replication (37). PNPT1 prevents dsRNA formation (38). Based on the above evidence, the present study hypothesized that low expression of the aforementioned genes helps the host obtain a higher viral load. A study has shown that the TRIM38 is an important member of the antiviral network of the interferon family, which can activate the promoter of interferon β (39). IRF7 is an important bridge connecting interferon-mediated responses in virus-induced asthma deteriorations (14). The present study demonstrated that IFIH1 was significantly downregulated in the acute phase of RV-induced asthma deterioration, which was consistent with the aforementioned report (32) and further confirmed the role of the interferon family in anti-rhinovirus infection.

TFs are the regulatory factors of gene expression and are closely associated with the occurrence and development of human diseases. In the present study, GATA2 and CREB1 were found to be the most important TFs regulating hub genes. GATA2 is essential for the survival and renewal of hematopoietic stem cells and interacts with a variety of TFs (40). GATA2

deficiency can cause a variety of immune cell disorders and increase virus susceptibility (41). CREB1, a member of the CREB/activating TF protein family, is involved in the transcriptional regulation of various viruses, including hepatitis B (42). A study has shown that IL-6 mediated the interaction between CREB1 and STAT1 in adrenal medulla chromaffin cells to regulate the release of cytokines and inflammatory mediators (43). Furthermore, the present study identified 25 miRNAs that regulate hub genes, such as miR-146a-5p and miR-424-5p. In diabetic nephropathy, miR-146a-5p can activate the STAT1 signaling pathway and promote M2-type macrophage polarization to enhance anti-inflammatory effects and improve renal function (44). In the course of dengue virus infection, miR-146a-5p is considered to be an important molecule regulating the expression of STAT1 and ISG15 (45). Additionally, miR-424-5p serves an important role in inhibiting hepatitis B virus (HBV) infection and the progression of HBV-related hepatocellular carcinoma (46). In the present study, IFIH1 regulated by miR-424-5p (Fig. 6) and enriched in the hepatitis B signaling pathway, which supports the aforementioned report.

Our previous study demonstrated that the potential of SARS-CoV-2 to induce asthma exacerbation was similar to that of rhinovirus (47). Importantly, the hub genes for asthma deterioration induced by both viruses were nearly the same. This suggested that asthma deteriorations induced by different respiratory viruses may have the same mechanism, which provides a potential therapeutic target for asthma deteriorations induced by mixed viral infections. In addition, the signaling pathways associated with the cDEGs of the two dataset pairs also overlapped (for example, 'Influenza A' and 'NOD-like receptor signaling pathway' were identified in both studies). However, the key modules of asthma deterioration induced by these two respiratory viruses are different: The IRG1/BATF2 module was dominated by RV, and the TRIM38/GBP3 module was dominated by SARS-CoV-2 (47).

In conclusion, in the present study, the cDEGs of RV ssRNA and dsRNA-induced asthma deteriorations were screened using the GSE51392 and GSE30326 datasets. On this basis, the mechanisms of asthma deterioration induced by ssRNA and dsRNA were systematically studied at the molecular, signaling pathway and interaction network levels. GO-KEGG enrichment analysis and identification of key modules showed that the hub genes STAT1, IFIH1, IRF7, DDX58 and ISG15 are considered to serve an important role in the progression of RV ssRNA and dsRNA-induced asthma deterioration. At the pathway level, 'influenza A', and TLR signaling pathway suggest that inflammatory factor expression and antiviral effects serve a major role in innate immunity. From an interaction network perspective, a key module with STAT1 as the core was identified. Finally, the molecules and drugs that regulate cDEGs (including hub genes) were analyzed and key hub genes (STAT1 and IFIH1) were verified using RT-qPCR. It is expected that the aforementioned findings will contribute to an improved understanding of the molecular mechanisms of RV-induced asthma deterioration.

However, the present study had certain limitations. First, the two datasets analyzed in the present study were from different age groups, which may have influenced the results. Secondly, clinical samples were collected from patients with RV-induced asthma deteriorations for self-paired comparison, but a control group of healthy children was not included.

Acknowledgements

Not applicable.

Funding

The present study was supported by the Science Foundation of Wuhu Science and Technology Bureau (grant no. WH2022226).

Availability of data and materials

Both datasets involved in this study are available for download from the GEO database with the accession numbers of GSE30326 and GSE51392 (https://www.ncbi.nlm.nih.gov/geo/).

Authors' contributions

QA and XZ conceived the idea, collected clinical samples and wrote the manuscript. WG, YC and ZJ produced the figures and analyzed data. HLu and HLi contributed to visualization and performed qPCR. XZ contributed to overall editing and supervision. All authors read and approved the final version of the manuscript. QA and XZ confirm the authenticity of all the raw data.

Ethics approval and consent to participate

The present study was performed in line with the principles of The Declaration of Helsinki. The patients and their guardians provided written informed consent for participation in the study. The present study was approved by the Ethics Committee of Wuhu Hospital of Traditional Chinese Medicine (approval no. 20220430; Wuhu, China).

Patient consent for publication

All patients and their guardians provided written informed consent for publication.

Competing interests

The authors declare that they have no competing interests.

References

1. Helou DG, Shafiei-Jahani P, Lo R, Howard E, Hurrell BP, Galle-Treger L, Painter JD, Lewis G, Soroosh P, Sharpe AH and Akbari O: PD-1 pathway regulates ILC2 metabolism and PD-1 agonist treatment ameliorates airway hyperreactivity. Nat Commun 11: 3998, 2020.
2. Cho JL, Ling MF, Adams DC, Faustino L, Islam SA, Afshar R, Griffith JW, Harris RS, Ng A, Radicioni G, *et al*: Allergic asthma is distinguished by sensitivity of allergen-specific CD4+ T cells and airway structural cells to type 2 inflammation. Sci Transl Med 8: 359ra132, 2016.
3. Zhu Z, Lee PH, Chaffin MD, Chung W, Loh PR, Lu Q, Christiani DC and Liang L: A genome-wide cross-trait analysis from UK Biobank highlights the shared genetic architecture of asthma and allergic diseases. Nat Genet 50: 857-864, 2018.

4. Garcia-Marcos L, Asher MI, Pearce N, Ellwood E, Bissell K, Chiang CY, El Sony A, Ellwood P, Marks GB, Mortimer K, *et al*: The burden of asthma, hay fever and eczema in children in 25 countries: GAN Phase I study. Eur Respir J 60: 2102866, 2022.
5. Mortimer K, Reddel HK, Pitrez PM and Bateman ED: Asthma management in low and middle income countries: Case for change. Eur Respir J 60: 2103179, 2022.
6. Toussaint M, Jackson DJ, Swieboda D, Guedan A, Tsourouktsoglou TD, Ching YM, Radermecker C, Makrinioti H, Aniscenko J, Bartlett NW, *et al*: Host DNA released by NETosis promotes rhinovirus-induced type-2 allergic asthma exacerbation. Nat Med 23: 681-691, 2017.
7. Michi AN, Love ME and Proud D: Rhinovirus-Induced modulation of epithelial phenotype: Role in Asthma. Viruses 12: 1328, 2020.
8. Han M, Rajput C, Hinde JL, Wu Q, Lei J, Ishikawa T, Bentley JK and Hershenson MB: Construction of a recombinant rhinovirus accommodating fluorescent marker expression. Influenza Other Respir Viruses 12: 717-727, 2018.
9. Niespodziana K, Stenberg-Hammar K, Megremis S, Cabauatan CR, Napora-Wijata K, Vacal PC, Gallerano D, Lupinek C, Ebner D, Schlederer T, *et al*: PreDicta chip-based high resolution diagnosis of rhinovirus-induced wheeze. Nat Commun 9: 2382, 2018.
10. Bochkov YA, Watters K, Ashraf S, Griggs TF, Devries MK, Jackson DJ, Palmenberg AC and Gern JE: Cadherin-related family member 3, a childhood asthma susceptibility gene product, mediates rhinovirus C binding and replication. P Natl Acad Sci USA 112: 5485-5490, 2015.
11. Mehta AK, Doherty T, Broide D and Croft M: Tumor necrosis factor family member LIGHT acts with IL-1β and TGF-β to promote airway remodeling during rhinovirus infection. Allergy 73: 1415-1424, 2018.
12. Wang Q, Nagarkar DR, Bowman ER, Schneider D, Gosangi B, Lei J, Zhao Y, McHenry CL, Burgens RV, Miller DJ, *et al*: Role of double-stranded RNA pattern recognition receptors in rhinovirus-induced airway epithelial cell responses. J Immunol 183: 6989-6997, 2009.
13. Ganjian H, Rajput C, Elzoheiry M and Sajjan U: Rhinovirus and innate immune function of airway epithelium. Front Cell Infect Microbiol 10: 277, 2020.
14. Bosco A, Ehteshami S, Panyala S and Martinez FD: Interferon regulatory factor 7 is a major hub connecting interferon-mediated responses in virus-induced asthma exacerbations in vivo. J Allergy Clin Immunol 129: 88-94, 2012.
15. Wagener AH, Zwinderman AH, Luiten S, Fokkens WJ, Bel EH, Sterk PJ, and van Drunen CM: dsRNA-induced changes in gene expression profiles of primary nasal and bronchial epithelial cells from patients with asthma, rhinitis and controls. Respir Res 15: 9, 2014.
16. Zhu X, Tang LP, Mao J, Hameed Y, Zhang J, Li N, Wu D, Huang Y and Li C: Decoding the Mechanism behind the Pathogenesis of the Focal Segmental Glomerulosclerosis. Comput Math Method Med 2022: 1941038, 2022.
17. Wesolowska-Andersen A, Everman JL, Davidson R, Rios C, Herrin R, Eng C, Janssen WJ, Liu AH, Oh SS, Kumar R, *et al*: Dual RNA-seq reveals viral infections in asthmatic children without respiratory illness which are associated with changes in the airway transcriptome. Genome Biol 18: 12, 2017.
18. Livak KJ and Schmittgen TD: Analysis of relative gene expression data using real-time quantitative PCR and the 2(-Delta Delta C(T)) Method. Methods 25: 402-408, 2001.
19. Thompson EA, Sayers BC, Glista-Baker EE, Shipkowski KA, Ihrie MD, Duke KS, Taylor AJ and Bonner JC: Role of signal transducer and activator of transcription 1 in murine allergen-induced airway remodeling and exacerbation by carbon nanotubes. Am J Respir Cell Mol Biol 53: 625-636, 2015.
20. Kang YH, Biswas A, Field M and Snapper SB: STAT1 signaling shields T cells from NK cell-mediated cytotoxicity. Nat Commun 10: 912, 2019.
21. Jewell NA, Cline T, Mertz SE, Smirnov SV, Flano E, Schindler C, Grieves JL, Durbin RK, Kotenko SV and Durbin JE: Lambda interferon is the predominant interferon induced by influenza A virus infection in vivo. J Virol 84: 11515-11522, 2010.
22. Luu K, Greenhill CJ, Majoros A, Decker T, Jenkins BJ and Mansell A: STAT1 plays a role in TLR signal transduction and inflammatory responses. Immunol Cell Biol 92: 761-769, 2014.
23. Matsuyama T, Kubli SP, Yoshinaga SK, Pfeffer K and Mak TW: An aberrant STAT pathway is central to COVID-19. Cell Death Differ 27: 3209-3225, 2020.
24. LeMessurier KS, Rooney R, Ghoneim HE, Liu BM, Li K, Smallwood HS and Samarainghe AE: Influenza A virus directly modulates mouse eosinophil responses. J Leukoc Biol 108: 151-168, 2020.
25. Mu X and Hur S: Immunogenicity of In Vitro-Transcribed RNA. Acc Chem Res 54: 4012-4023, 2021.
26. Yan K, Zhu W, Yu L, Li N, Zhang X, Liu P, Chen Q, Chen Y and Han D: Toll-like receptor 3 and RIG-I-like receptor activation induces innate antiviral responses in mouse ovarian granulosa cells. Mol Cell Endocrinol 372: 73-85, 2013.
27. Amado-Rodriguez L, Salgado Del Riego E, Gomez de Ona J, López Alonso I, Gil-Pena H, Lopez-Martinez C, Martin-Vicente P, Lopez-Vazquez A, Gonzalez Lopez A, Cuesta-Llavona E, *et al*: Effects of IFIH1 rs1990760 variants on systemic inflammation and outcome in critically ill COVID-19 patients in an observational translational study. Elife 11: e73012, 2022.
28. Dieter C, de Almeida Brondani L, Lemos NE, Schaeffer AF, Zanotto C, Ramos DT, Girardi E, Pellenz FM, Camargo JL, Moresco KS, *et al*: Polymorphisms in ACE1, TMPRSS2, IFIH1, IFNAR2, and TYK2 genes are associated with worse clinical outcomes in COVID-19. Genes (Basel) 14: 29, 2022.
29. Wang P, Yang L, Cheng G, Yang G, Xu Z, You F, Sun Q, Lin RT, Fikrig E and Sutton RE: UBXN1 interferes with Rig-I-like receptor-mediated antiviral immune response by targeting MAVS. Cell Rep 3: 1057-1070, 2013.
30. Pugh C, Kolaczkowski O, Manny A, Korithoski B and Kolaczkowski B: Resurrecting ancestral structural dynamics of an antiviral immune receptor: Adaptive binding pocket reorganization repeatedly shifts RNA preference. BMC Evol Biol 16: 241, 2016.
31. Loske J, Rohmel J, Lukassen S, Stricker S, Magalhães VG, Liebig J, Chua RL, Thürmann L, Messingschlager M, Seegebarth A, *et al*: Pre-activated antiviral innate immunity in the upper airways controls early SARS-CoV-2 infection in children. Nat Biotechnol 40: 319-324, 2022.
32. Selinger C, Tisoncik-Go J, Menachery VD, Agnihothram S, Law GL, Chang J, Kelly SM, Sova P, Baric RS and Katze MG: Cytokine systems approach demonstrates differences in innate and pro-inflammatory host responses between genetically distinct MERS-CoV isolates. BMC Genomics 15: 1161, 2014.
33. Rachmiel M, Bloch O, Bistritzer T, Weintrob N, Ofan R, Koren-Morag N and Rapoport MJ: TH1/TH2 cytokine balance in patients with both type 1 diabetes mellitus and asthma. Cytokine 34: 170-176, 2006.
34. Zhu J, Message SD, Mallia P, Kebadze T, Contoli M, Ward CK, Barnathan ES, Mascelli MA, Kon OM, Papi A, *et al*: Bronchial mucosal IFN-α/β and pattern recognition receptor expression in patients with experimental rhinovirus-induced asthma exacerbations. J Allergy Clin Immunol 143: 114-125 e4, 2019.
35. Gill MA, Bajwa G, George TA, Dong CC, Dougherty II, Jiang N, Gan VN and Gruchalla RS: Counterregulation between the FcepsilonRI pathway and antiviral responses in human plasmacytoid dendritic cells. J Immunol 184: 5999-6006, 2010.
36. Liu T, Zhou YT, Wang LQ, Li LY, Bao Q, Tian S, Chen MX, Chen HX, Cui J and Li CW: NOD-like receptor family, pyrin domain containing 3 (NLRP3) contributes to inflammation, pyroptosis, and mucin production in human airway epithelium on rhinovirus infection. J Allergy Clin Immunol 144: 777-787 e9, 2019.
37. Grünvogel O, Esser-Nobis K, Reustle A, Schult P, Müller B, Metz P, Trippler M, Windisch MP, Frese M, Binder M, *et al*: DDX60L is an interferon-stimulated gene product restricting hepatitis C virus replication in cell culture. J Virol 89: 10548-10568, 2015.
38. Wolin SL and Maquat LE: Cellular RNA surveillance in health and disease. Science 366: 822-827, 2019.
39. Kane M, Zang TM, Rihn SJ, Zhang FW, Kueck T, Alim M, Schoggins J, Rice CM, Wilson SJ and Bieniasz PD: Identification of interferon-stimulated genes with antiretroviral activity. Cell Host Microbe 20: 392-405, 2016.
40. Cohen JI: GATA2 deficiency and epstein-barr virus disease. Front Immunol 8: 1869, 2017.
41. Spinner MA, Sanchez LA, Hsu AP, Shaw PA, Zerbe CS, Calvo KR, Arthur DC, Gu W, Gould CM, Brewer CC, *et al*: GATA2 deficiency: A protean disorder of hematopoiesis, lymphatics, and immunity. Blood 123: 809-821, 2014.
42. Zhao X, Fan H, Chen X, Zhao X, Wang X, Feng YJ, Liu M, Li S and Tang H: Hepatitis B Virus DNA polymerase restrains viral replication through the CREB1/HOXA distal transcript antisense RNA Homeobox A13 Axis. Hepatology 73: 503-519, 2021.

43. Jenkins DE, Sreenivasan D, Carman F, Samal B, Eiden LE and Bunn SJ: Interleukin-6-mediated signaling in adrenal medullary chromaffin cells. J Neurochem 139: 1138-1150, 2016.
44. Zhang Y, Le X, Zheng S, Zhang K, He J, Liu M, Tu C, Rao W, Du H, Ouyang Y, *et al*: MicroRNA-146a-5p-modified human umbilical cord mesenchymal stem cells enhance protection against diabetic nephropathy in rats through facilitating M2 macrophage polarization. Stem Cell Res Ther 13: 171, 2022.
45. Xie LM, Yin X, Bi J, Luo HM, Cao XJ, Ma YW, Liu YL, Su JW, Lin GL and Guo XG: Identification of potential biomarkers in dengue via integrated bioinformatic analysis. PLoS Negl Trop Dis 15: e0009633, 2021.
46. Chen Y, Li S, Wei Y, Xu Z and Wu X: Circ-RNF13, as an oncogene, regulates malignant progression of HBV-associated hepatocellular carcinoma cells and HBV infection through ceRNA pathway of circ-RNF13/miR-424-5p/TGIF2. Bosn J Basic Med Sci 21: 555-568, 2021.
47. Wei G, Yi C, Ziyun J, Hui L, Hui L and Yilong X: Network-Based analysis of the genetic effects of SARS-CoV-2 infection to patients with exacerbation of Virus-Induced Asthma (VAE). Research Square: https://doi.org/10.21203/rs.3.rs-948407/v1.